Articles

Optimization of Operation for Multiple Oxygen Burners in Industrial Furnaces

YAMAGUCHI Masashi*　MOROKUMA Akira**　KOBAYASHI Yu**

Industrial furnaces often operate multiple burners, where conventional tuning remains suboptimal and manual search becomes infeasible as the combinatorial space explodes. We built a data-driven framework based on Bayesian optimization to efficiently select operating conditions. First, computational fluid dynamics for a two-burner test furnace identified NOx-reducing settings with few trials. Next, we validated on a four-burner furnace. Despite the vastly larger search space, Bayesian optimization reached promising conditions rapidly. These results show that Bayesian optimization is effective for optimizing complex burner operations and has strong practical applicability.

1. Introduction

Industrial furnaces are widely used in materials industries such as iron and steel, glass, and non-ferrous metals to heat products during manufacturing. Many of these furnaces use burner combustion for product heating. CO_2 emissions from industrial furnaces are estimated at approximately 150 million tons per year and account for a substantial share of industrial emissions[1]. Accordingly, many companies are urgently considering measures to reduce these emissions.

Oxy-fuel combustion is a method that uses O_2 or oxygen-enriched air as the oxidizer instead of air. By eliminating N_2, which does not contribute to combustion, the heat released can be utilized more efficiently, thereby reducing fuel consumption. When hydrocarbon fuels are used, fuel consumption and CO_2 emissions can be reduced by up to 50% compared with conventional air-fuel combustion[2,3]. This technology has traditionally been used for cost reduction, but it has recently attracted renewed attention for CO_2 reduction.

However, one challenge of oxy-fuel combustion is thermal NOx formation caused by high flame temperatures. Even when pure O_2 is used, the oxidizer contains a small amount of N_2 from its production process, and air entrainment is unavoidable in practical furnaces. As a result, NOx emissions from oxy-fuel combustion can in some cases exceed those from air-fuel combustion.

To address this issue, oxygen burners incorporating the staged-combustion concept shown in Fig. 1 are widely used. In the first stage, a high-temperature but oxygen-deficient flame is formed. In the second stage, the remaining oxidizer is introduced while mixing with the furnace gas. This suppresses localized high-temperature regions and reduces NOx formation.

Although some small furnaces use a single burner, many industrial furnaces operate multiple burners. In particular, large reheating furnaces and glass-melting furnaces employ ten or more burners. In such multi-burner systems, adjustment of operating conditions is often limited to the heat input of each burner. In principle, however, further NOx reduction and a more desirable temperature distribution should be achievable by adjusting the equivalence ratio and oxidizer split ratio for each burner. As the number of burners increases, the number of possible operating-condition combinations grows rapidly, making manual optimization impractical. In addition, the introduction of alternative fuels such as H_2 and NH_3 is expected to further increase the number of adjustable parameters.

In this study, we investigated data-driven optimization of burner operating conditions using Bayesian optimization to efficiently search a large design space with a practical number of trials. First, we examined the feasibility of the approach through numerical simulation. We then validated its effectiveness experimentally.

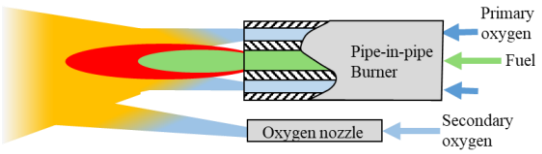

Fig. 1 The Oxygen burner for industrial furnaces

* R&D Administration Department, R&D Planning Division, R&D Unit
** Oxy-fuel Combustion Development Department, Yamanashi Technology Solution Center, R&D Unit

2. Bayesian Optimization

Bayesian optimization is a method for efficiently searching for high-performance solutions when evaluation of the objective function is expensive[4, 5]. It is widely used for tasks such as tuning hyperparameters of machine learning models and optimizing experimental conditions. The objective function is modeled using a probabilistic surrogate based on Gaussian processes, and the point that maximizes the acquisition function is selected as the next evaluation point. This enables efficient convergence for nonlinear and high-dimensional problems while balancing exploration and exploitation.

A Gaussian process is a model that represents uncertainty in a function by assuming that any finite set of its values follows a multivariate normal distribution. It is characterized by a mean function $\mu(x)$ and a covariance (kernel) function $k(x, x')$ as follows.

$$f(x) \sim GP(\mu(\boldsymbol{x}), k(\boldsymbol{x}, \boldsymbol{x}')) \quad (1)$$

The kernel function expresses the correlation between input points, and the kernel type strongly affects the performance of the Gaussian-process model. In this study, we used the radial basis function (RBF) kernel, a representative and widely used kernel, as follows.

$$k(\boldsymbol{x}, \boldsymbol{x}') = \sigma^2 \exp\left(-\frac{\|\boldsymbol{x} - \boldsymbol{x}'\|^2}{2l^2}\right) \quad (2)$$

Here, σ^2 is the variance and l is the length scale.

An acquisition function is used to determine the next evaluation point from the Gaussian-process model. Among various acquisition functions, we adopted the Expected Improvement (EI), which estimates the expected amount of improvement for maximization problems, as follows.

$$EI(x) = \boldsymbol{E}[max(0, f(x) - f^*)] = (\mu(x) - f^*)\Phi(Z) + \sigma(x)\phi(Z) \quad (3)$$

Here, f^* is the best observed value, $\mu(x)$ is the predictive mean, and $\sigma(x)$ is the predictive standard deviation. Φ and ϕ denote the cumulative distribution function and probability density function of the standard normal distribution, respectively. Z is defined as $Z = (\mu(x) - f^*)/\sigma(x)$. For minimization problems, the objective can be reformulated into a maximization problem by sign inversion.

In this study, we implemented the Bayesian optimization algorithm in Python using the open-source library BoTorch 0.14.0 [6], which provides Gaussian-process models, kernel functions, and acquisition functions required for the optimization.

3. Verification through Numerical Simulation

3.1 Fluid Dynamics Model

To verify the effectiveness of Bayesian optimization, we conducted numerical simulations using an existing combustion test furnace. The furnace analyzed in this study is a rectangular refractory-lined test furnace, as shown in Fig. 2. In this simulation, two burners were installed on the side wall, and combustion gas was discharged through a single flue. The burners were of a staged-combustion type. Each burner consisted of a pipe-in-pipe main burner and a single-pipe oxygen nozzle. Fuel was supplied through the inner pipe of the pipe-in-pipe burner, while part of the oxidizer was supplied through the outer pipe to form a high-temperature, oxygen-deficient flame. The remaining oxidizer was then supplied through the oxygen nozzle and mixed with the furnace gas to complete combustion.

Table 1 summarizes the main numerical models used in the simulation. We used the commercial CFD solver Simcenter STAR-CCM+, and the analysis was performed under steady-state conditions. Combustion was modeled using a chemical

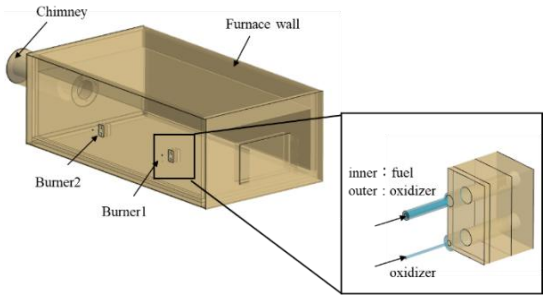

Fig. 2 Computational domain of test furnace

Table 1 Calculation model

Category	Model / Setting
Analysis type	Steady state
Combustion model	Flamelet approach - Chemical equilibrium model + Extended Zeldovich mechanism
Reaction mech.	GRI Mech 3.0
Turbulent model	Realizable k-ε model + Blended wall function
Radiation model	Discrete Ordinate method + WSGG model
Fuel	CH_4
Oxidizer	O_2 95vol% + N_2 5vol%

equilibrium model based on a non-premixed flamelet approach, and thermophysical properties were taken from the GRI-Mech 3.0 database. NOx species were not included in the flamelet PDF table. Instead, thermal NOx was calculated in post-processing using the extended Zeldovich mechanism. The turbulence model was the realizable k-ε model with a mixed wall function treatment near the walls. Radiative heat transfer was analyzed using the Discrete Ordinates (DO) method, and gas radiation was modeled using the Weighted Sum of Gray Gases Model (WSGGM), with the contributions of H_2O and CO_2 estimated from Hottel's charts. The fuel was CH_4, and the oxidizer consisted of 95 vol% O_2 and 5 vol% N_2. Thermal boundary conditions accounting for heat loss by convection and radiation were applied to the outer surfaces of the furnace walls.

3.2 Operating Range and Optimization Setup

Table 2 shows the input variables and the objective function. The input variables were heat input, oxygen ratio, and staging ratio. The heat input was calculated from the fuel flow rate based on the lower heating value. The oxygen ratio is defined as the reciprocal of the equivalence ratio and represents the ratio of supplied oxygen to the amount required for complete combustion. The staging ratio is defined as the fraction of the oxidizer flow for each burner that is directed to the oxygen nozzle. The total heat input of the two burners was fixed at 100 kW. Each burner could take values from 30 to 70 kW in increments of 5 kW. The heat input of Burner 1 was treated as an independent variable, and that of Burner 2 was determined accordingly. The oxygen ratio of Burner 1 was varied from 0.8 to 1.2 in increments of 0.02, and that of Burner 2 was calculated so that the overall oxygen ratio was maintained at 1.02. The staging ratio was specified independently for each burner and ranged from 0.3 to 0.8 in increments of 0.05. In total, 4 independent variables and 2 dependent variables were considered, giving 6 variables and 22869 possible combinations. The objective function was the NO mole fraction in the flue gas, and the optimization searched for the combination of operating conditions that minimized this value. To match the measurement conditions, the NO mole fraction was evaluated on a dry basis.

Fig. 3 shows the optimization procedure. First, 5 initial data points were prepared (Table 3), and CFD simulations were performed for each condition. A Gaussian process regression model was then constructed from the resulting data, and the next evaluation point was selected from the untested candidates using an acquisition function. A simulation was performed for the selected condition, the data were added to the dataset, and the model was reconstructed. After the initial dataset had been prepared, this cycle of model reconstruction and selection of the next point was repeated automatically without human intervention. No explicit stopping criterion was defined in this study, and the search was terminated after a total of 25 conditions while checking the optimization progress.

Table 2 Variables

Type	Variables
Input variables	Heat input from burner1
	Heat input from burner2
	Oxygen ratio of burner1
	Oxygen ratio of burner2
	Staging ratio of burner1
	Staging ratio of burner2
Objective function	NO (dry gas of flue gas)

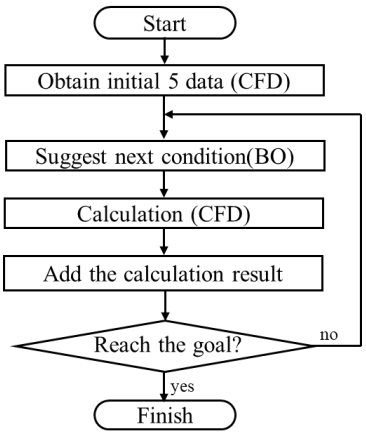

Fig. 3 Flowchart of Bayesian optimization

Table 3 Initial 5 conditions

Case No.	Burner1			Burner2		
	Heat input [kW]	O_2 ratio [-]	Staging ratio [-]	Heat input [kW]	O_2 ratio [-]	Staging ratio [-]
1	50	1.02	0.5	50	1.02	0.5
2	50	1.02	0.7	50	1.02	0.7
3	40	1.02	0.5	60	1.02	0.5
4	50	0.86	0.75	50	1.18	0.75
5	50	0.92	0.75	50	1.12	0.75

3.3 Results and Discussion

To examine the flame appearance under the initial conditions, the temperature field for Case 1 was visualized by volume rendering, as shown in Fig. 4. Figure 5 shows the temperature distributions in vertical cross-sections through the centers of Burners 1 and 2 for Case 1. Excluding the flame regions, the furnace temperature was generally in the range

of 1450°C to 1550°C. High-temperature regions were formed by combustion of the gases discharged from the pipe-in-pipe burners. Similarly, Fig. 6 shows the temperature distributions in vertical cross-sections of each burner for Case 2. Compared with Case 1, in which the staging ratio was 0.5, Case 2, with a staging ratio of 0.7, exhibited smaller high-temperature regions formed by the pipe-in-pipe burners. The oxidizer from the oxygen nozzles mixed with the furnace gas and merged with the unburned fuel. As a result, combustion proceeded more gradually, suppressing localized high-temperature regions throughout the furnace. This behavior is consistent with the design concept of the staged-combustion structure. The NO concentration in the flue gas decreased from 2905 ppm in Case 1 to 1833 ppm in Case 2. Although the absolute values may have been higher than the measured values because of limitations of the analysis model, we judged that the model captured the trends appropriately for relative comparison and therefore used it for subsequent data acquisition.

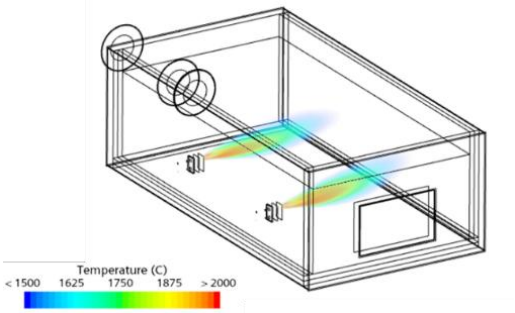

Fig. 4 Flame appearance by volume rendering of temperature

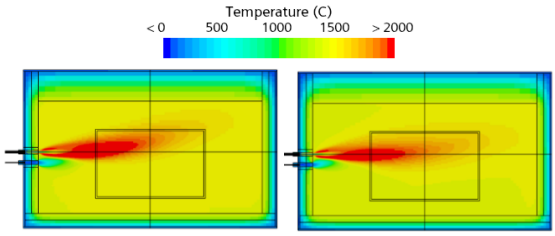

(a) Burner 1 (b) Burner 2

Fig. 5 Temperature distribution of case 1

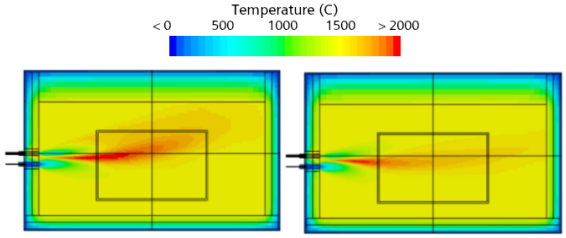

(a) Burner 1 (b) Burner 2

Fig. 6 Temperature distribution of case 2

Table 4 lists the simulation results. After the initial 5 conditions, the search continued until 25 conditions had been evaluated. Figure 7 shows the NO value obtained in each trial and the best value found up to that point. Although a relatively low NO value of 1380 ppm was obtained in the initial dataset, the best value was later improved to 1270 ppm at the 15th trial. Under this optimum condition, the oxygen ratios of Burners 1 and 2 were 0.82 and 1.22, respectively. As expected, the results showed that varying the oxygen ratio for each burner can reduce NO more effectively than the conventional operating method in which the oxygen ratio is fixed. The staging ratios under this condition also differed between the two burners, at 0.65 and 0.80. Reproducibility under actual operating conditions remains to be verified. Nevertheless, these results highlight an advantage of data-driven optimization. Manual condition setting often uses the same ratio for both burners, whereas the present approach identified non-intuitive conditions and confirmed their numerical effectiveness.

Table 4 Calculation result

No.	Burner1			Burner2			NO [ppm]
	Heat input [kW]	O_2 ratio [-]	Staging ratio [-]	Heat input [kW]	O_2 ratio [-]	Staging ratio [-]	
1	50	1.02	0.5	50	1.02	0.5	2905
2	50	1.02	0.7	50	1.02	0.7	1833
3	40	1.02	0.5	60	1.02	0.5	2329
4	50	0.86	0.75	50	1.18	0.75	1380
5	50	0.92	0.75	50	1.12	0.75	1650
6	50	0.8	0.7	50	1.24	0.75	1340
7	50	0.8	0.8	50	1.24	0.7	1580
8	50	0.8	0.8	50	1.24	0.8	1450
9	50	0.8	0.75	50	1.24	0.8	1380
10	50	0.82	0.55	50	1.22	0.8	1360
11	50	0.82	0.45	50	1.22	0.75	1520
12	50	0.82	0.65	50	1.22	0.75	1340
13	55	0.84	0.7	45	1.24	0.75	1420
14	45	0.8	0.65	55	1.2	0.8	1380
15	50	0.82	0.65	50	1.22	0.8	1270
16	45	1.16	0.8	55	0.906	0.75	1570
17	55	1.12	0.6	45	0.898	0.8	2360
18	35	1.12	0.8	65	0.966	0.7	1780
19	45	1.2	0.8	55	0.873	0.65	1740
20	40	1.14	0.5	60	0.94	0.75	1960
21	50	0.84	0.65	50	1.2	0.8	1280
22	55	0.88	0.65	45	1.191	0.8	1510
23	40	0.88	0.6	60	1.113	0.75	1690
24	65	0.8	0.45	35	1.429	0.8	1446
25	55	0.8	0.6	45	1.289	0.8	1420

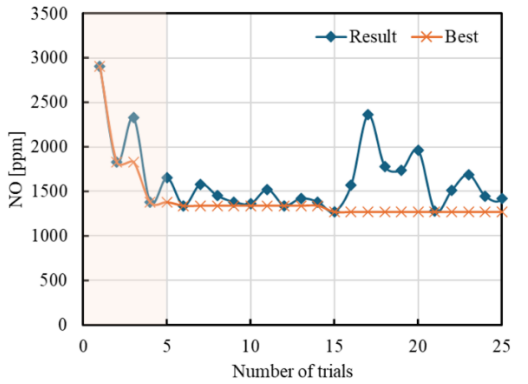

Fig. 7 Optimization progress

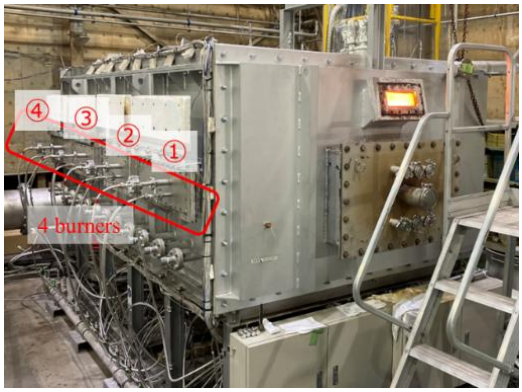

Fig. 8 Experimental furnace

4. Experimental Demonstration

4.1 Experimental Setup and Conditions

After confirming the effectiveness of Bayesian optimization through numerical simulation, we conducted an experimental demonstration. Figure 8 shows the furnace used in this study. This furnace is the one modeled in the previous section and employs the same staged-burner concept. For the demonstration test, however, 4 burners were installed. Multiple thermocouples are installed on the roof of the furnace to determine the temperature distribution over the inner roof surface. A portion of the flue gas is extracted from the chimney, and the gas composition, including NOx, is measured using a continuous gas analyzer. Table 5 shows the main experimental conditions. Natural gas was used as the fuel, and the oxidizer was a gas containing 93 vol% O_2, prepared by mixing pure O_2 and N_2. For Burners 1 to 3, the heat input was varied over 5 levels from 20 to 34 kW, and the oxygen ratio was varied over 5 levels from 0.8 to 1.2. The heat input and oxygen ratio of Burner 4 were determined so that the total heat input of the 4 burners was 96 kW and the overall oxygen ratio was 1.0. The staging ratio was set independently for each burner at 4 levels from 0.5 to 0.8. In total, 12 input variables were defined for the 4 burners, resulting in a search space of 624128 possible combinations. The optimization searched for the combination that minimized the NOx concentration in the flue gas. As in the CFD simulation, the Bayesian optimization cycle was started after the 5 predefined initial conditions had been evaluatedd (Table 6).

Table 5 Experimental Conditions

Category	Condition
Burner type	Pipe-in-pipe + Staging nozzle
Burner number	4
Fuel	Natural gas
Oxidizer	O_2 93vol% + N_2 7vol%
Heat input [kW]	20, 24, 27, 31, 34 (Total is 96 kW)
Oxygen ratio [-]	0.8, 0.9, 1.0, 1.1, 1.2 (Total is 1.0)
Staging ratio [-]	0.5, 0.6, 0.7, 0.8

Table 6 Initial 5 experimental conditions

Case No.		1	2	3	4	5
Burner 1	Heat input [kW]	24	20	20	20	20
	O_2 ratio[-]	1.0	0.9	0.8	1.2	1.2
	Staging ratio[-]	0.8	0.5	0.6	0.7	0.5
Burner 2	Heat input [kW]	24	24	20	20	31
	O_2 ratio[-]	1.0	0.8	1.1	0.9	0.9
	Staging ratio [-]	0.8	0.7	0.5	0.5	0.7
Burner 3	Heat input [kW]	24	20	34	24	20
	O_2 ratio[-]	1.0	1.2	1.1	0.8	1.0
	Staging ratio [-]	0.8	0.5	0.7	0.6	0.7
Burner 4	Heat input [kW]	24	32	22	32	25
	O_2 ratio[-]	1.0	1.09	0.94	1.09	0.96
	Staging ratio [-]	0.8	0.5	0.6	0.5	0.7

4.2 Experimental Resultsnditions

Among the initial conditions, Case 1 was defined as the standard condition, with all 4 burners set to a heat input of 24 kW, an oxygen ratio of 1.0, and a staging ratio of 0.8. This is a representative operating condition selected by conventional adjustment methods. For Case 1, the temperature on the inner roof surface ranged from 1300°C to 1400°C, with an average of 1353°C (Fig. 9). This was more than 100°C lower than the temperature assumed in the CFD simulation. As a result, the NOx concentration in the flue gas was as low as 157 ppm.

Figure 10 shows the results of the Bayesian optimization cycle using the 5 initial conditions, including the standard condition, as the initial dataset. Although low NOx values had already been obtained in the initial dataset, the best value of 75 ppm was subsequently achieved in Case 15. Despite the much larger search space than in the previous section, a promising condition was identified with a small number of trials.

Table 7 lists the NOx values and operating conditions for the standard Case 1, Case 5, which showed a relatively high NOx value, and Case 15, which gave the best result. Figure 11 shows the temperature distributions on the inner roof surface for Cases 5 and 15. In Case 5, Burner 1 on the upstream side relative to the flue was in an oxygen-rich condition, and Burner 2 was operated at the maximum heat input. As a result, the maximum roof temperature appeared on the upstream side, and the NOx generated there likely had a major influence on the concentration measured at the flue.

In contrast, in Case 15, Burners 1 and 2 on the upstream side were operated under fuel-rich conditions, while the downstream side of the furnace was oxygen-rich to complete combustion. This indicates that staged combustion was achieved across the entire furnace, which is considered to have greatly suppressed NOx formation. These results show that Bayesian optimization alone can autonomously identify practically reasonable operating conditions. In addition to demonstrating its usefulness as an operational optimization method, the results also indicate strong potential for future automation.

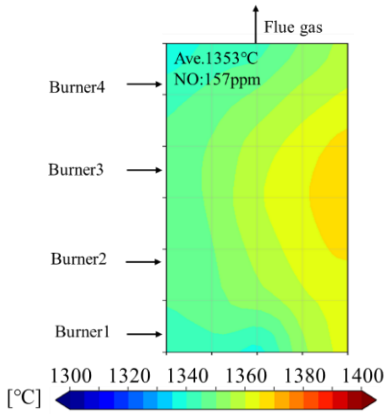

Fig. 9 Tempreture distributions on roof surface (Case1)

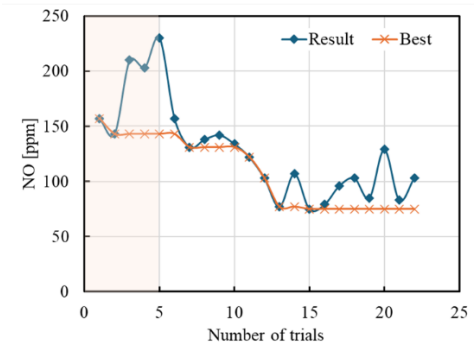

Fig. 10 Optimization progress in experiments

Table 7 Typical results

Case No.		1	5	15
NOx[ppm]		157	230	75
Burner1	Heat input [kW]	24	20	24
	O_2 ratio[-]	1.0	1.2	0.8
	Staging ratio [-]	0.8	0.5	0.8
Burner2	Heat input [kW]	24	31	20
	O_2 ratio[-]	1.0	0.9	0.8
	Staging ratio [-]	0.8	0.7	0.8
Burner3	Heat input [kW]	24	20	20
	O_2 ratio[-]	1.0	1.0	1.2
	Staging ratio [-]	0.8	0.7	0.8
Burner4	Heat input [kW]	24	25	32
	O_2 ratio[-]	1.0	0.964	1.15
	Staging ratio [-]	0.8	0.7	0.8

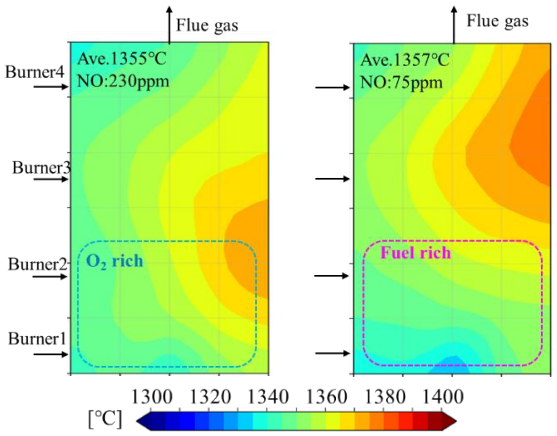

(a) Case No.5 (b) Case No.15

Fig. 11 Tempreture distributions on roof surface (Case5, 15)

5. Conclusion

In this study, we examined the use of Bayesian optimization to optimize the operating conditions for multiple oxygen burners. We first evaluated the method through CFD simulation and then demonstrated its applicability experimentally.

In the numerical study, Bayesian optimization was combined with CFD simulation to identify operating conditions that minimized the NO concentration in the flue gas. As a result, a reduction in NO that could not be achieved through conventional adjustment methods was obtained with a small number of trials. In particular, the NO concentration was minimized under conditions where the staging ratios differed between the two burners. Because such conditions would not normally be selected in conventional operation, this result highlights the usefulness of Bayesian optimization.

The experimental demonstration then verified the method for the 4-burner system, which involved a much larger search space of 624128 possible combinations. Even so, operating

conditions that further reduced NOx were identified with a small number of trials.

These findings demonstrate the practical applicability of Bayesian optimization to oxygen-burner operation. Based on these results, we plan to expand its internal use. We also plan to further improve the optimization algorithm so that it can handle larger numbers of input variables and support multi-objective optimization. The method has the potential to improve work efficiency by reducing the number of trials required during development. In addition, when combined with numerical simulation, it can be used to investigate suitable operating patterns before implementation in actual equipment. Ultimately, we aim to integrate this method with furnace control systems so that it can provide automated and autonomous optimization control.

References

1) National Institute for Environmental Studies, Japan, Greenhouse Gas Emissions Data of Japan (Fiscal Year 2022 Final Figures), 2024
2) N. Kobayashi, Taiyo Nippon Sanso Technical Report, No. 40, pp. 1-13, 2021
3) Y. Hagiwara and Y. Yamamoto, Journal of the Combustion Society of Japan, Vol. 67, pp. 26-33, 2025
4) B. Shahriari, K. Swersky, Z. Wang, R. P. Adams and N. de Freitas, Proc. of the IEEE, vol. 104, 1, 148-175, 2016
5) H. Imamura and K. Matsui, Bayesian Optimization: Fundamentals and Practice of Adaptive Experimental Design, 2023
6) Balandat, M., Karrer, B., Jiang, D. R., Daulton, S., Letham, B., Wilson, A. G., & Bakshy, E., NeurIPS, 2020